**-Electronic Supplementary Information-**
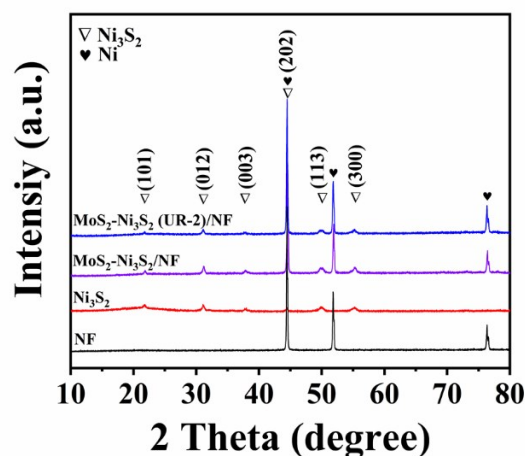


**Figure S1**. XRD patterns of NF, $Ni_3S_2$, $MoS_2$-$Ni_3S_2$/NF, $MoS_2$-$Ni_3S_2$ (UR-2)/NF.
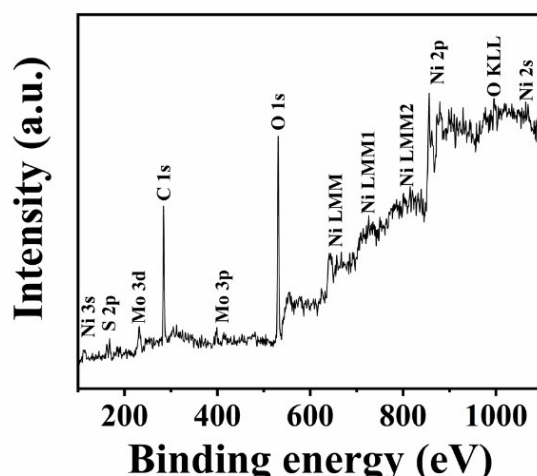


**Figure S2.** XPS survey spectra of $MoS_2$-$Ni_3S_2$ (UR-2)/NF.

**Table S1.** Comparison of HER activity of the $MoS_2$-$Ni_3S_2$ (UR-2)/NF with that of some recently reported non-precious electrocatalysts in alkaline media.

| Catalysts | $\eta_{10}$(mV) | $\eta_{100}$ (mV) | Tafel Slope (mV dec$^{-1}$) | Electrolyte | Ref. |
|---|---|---|---|---|---|
| $MoS_2$-$Ni_3S_2$ (UR-2)/NF | 98 | 191 | 74.8 | 1.0 M KOH | This work |
| $Ni_3S_2$ particles | 335 | -- | 97 | 1.0 M KOH | 1 |
| Laser-treated $MoS_2$ | 271 | -- | 74.5 | 1.0 M KOH | 2 |

| | | | | | |
|---|---|---|---|---|---|
| Co-Ni$_3$S$_2$/NF | 240 | ~370 | 144.99 | 1.0 M KOH | 3 |
| Ni$_3$S$_2$/Ni foam | 123 | 260 | 110 | 1.0 M KOH | 4 |
| MoS$_2$/Ni$_3$S$_2$ heterostructures | 110 | -- | 83 | 1.0 M KOH | 5 |
| NiSe$_2$ nanosheets | 184 | -- | 184 | 1.0 M KOH | 6 |
| V−Ni$_3$S$_2$−NW | 68 | 350 | 112 | 1.0 M KOH | 7 |
| N dope Ni$_3$S$_2$ | 155 | ~305 | 113 | 1.0 M KOH | 8 |
| Ni$_3$S$_2$ NWs | 199.2 | -- | 106.1 | 1.0 M KOH | 9 |
| Co$_9$S$_8$ Ni$_3$S$_2$ HNTs/Ni | 85 | ~235 | 83.1 | 1.0 M KOH | 10 |
| Ni$_3$S$_2$@MoS$_x$/NiO | 118 | ~256 | 65 | 1.0 M KOH | 11 |
| Ni-Fe/nanocarbon | 219 | -- | 110 | 1.0 M KOH | 12 |
| Co/β-Mo$_2$C@N-CNTs | 170 | -- | 92 | 1.0 M KOH | 13 |
| O-CoMoS nanosheet | 97 | 206 | 70 | 1.0 M KOH | 14 |
| G-Mo-Ni$_3$S$_2$-2/NF | 68 | ~220 | 68 | 1.0 M KOH | 15 |
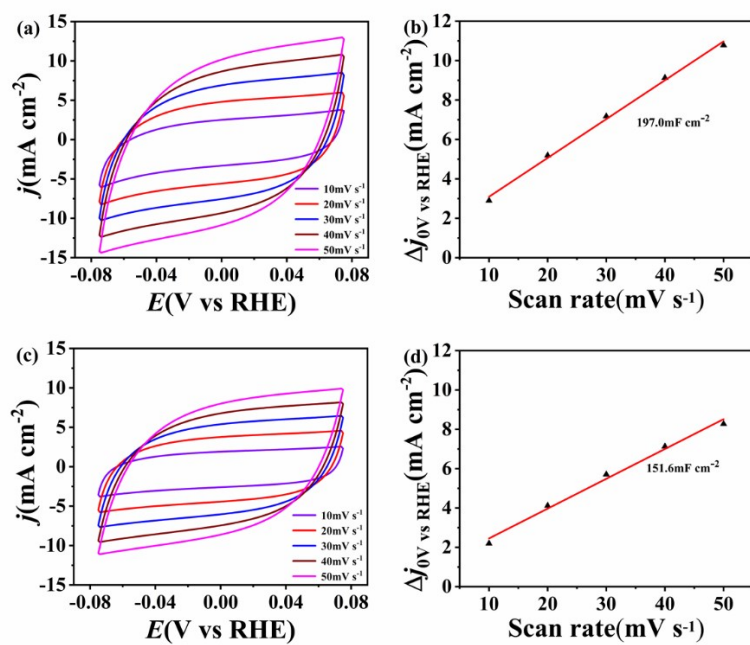


**Figure S3**. Cyclic voltammograms of (a) MoS$_2$-Ni$_3$S$_2$ (UR-2)/NF and (c) MoS$_2$-Ni$_3$S$_2$/NF. Estimation of C$_{dl}$ value (b) MoS$_2$-Ni$_3$S$_2$ (UR-2)/NF and (d) MoS$_2$-Ni$_3$S$_2$/NF.

The $C_{dl}$ values of all catalysts can be calculated by the half of the slope of the capacitive current versus scan rate, which is by plotting the current density variation ($\Delta j = (j_a - j_c)/2$) at 0 mV vs RHE ($j_a$ and $j_c$ represent current density of anode and cathode, respectively.). Data obtained from the cyclic voltammogram in Figure S4 (a) and (c)).

**Table S2.** Calculated double layer capacitance ($C_{dl}$) and electrochemical active surface area (ECSA)

| Catalysts | $C_{dl}$ (mF cm$^{-2}$) | ECSA (cm$^2$) |
|---|---|---|
| MoS$_2$-Ni$_3$S$_2$ /NF | 151.6 | 3790 |
| MoS$_2$-Ni$_3$S$_2$ (UR-2)/NF | 197.0 | 4925 |

Generally, the higher the double-layer capacitance ($C_{dl}$) value, the more active sites on the surface of the electrocatalyst. The $C_{dl}$ value is directly proportional to the electrochemical active surface area (ECSA), which can provide a relative comparison for average active sites on the area of the surface of the electrocatalyst. The calculation equation is as follows:

$$ECSA= C_{dl} / 40 \ \mu F$$

The $C_{dl}$ value is obtained through Figure S4 b and d. The capacitance of atomically smooth planar surface in 1.0 M KOH electrolyte ranges from 20 to 60 $\mu F$ cm$^{-2}$. For calculation, the area normalized specific capacitance was taken to be 40 $\mu F$ cm$^{-2}$.
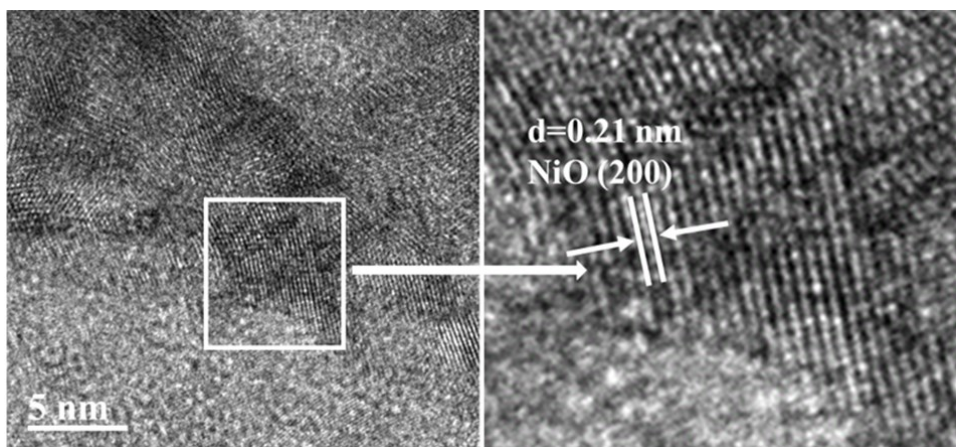
**Figure S4.** HR-TEM images of $MoS_2$-$Ni_3S_2$ (UR-2)/NF after OER test.

**Table S3.** Comparison of OER activity of the $MoS_2$-$Ni_3S_2$ (UR-2)/NF with that of some recently reported non-precious electrocatalysts in alkaline media.

| Catalysts | $\eta_{100}$ (mV) | Tafel Slope (mV dec$^{-1}$) | Electrolyte | Ref. |
|---|---|---|---|---|
| $MoS_2$-$Ni_3S_2$ (UR-2)/NF | 355 | 97.4 | 1.0 M KOH | This work |
| G-Mo-$Ni_3S_2$-2/NF | ~415 | 69 | 1.0 M KOH | 15 |
| Mo-Ni-Se@NF | 397 | 44.9 | 1.0 M KOH | 16 |
| Co-$MoS_{1+X}Se_{1+Y}$1-5 | ~450 | 71 | 1.0 M KOH | 17 |
| Zn-CoNiP/NF | ~380 | 51 | 1.0 M KOH | 18 |
| NiCoP NWAs/NF | 370 | 116 | 1.0 M KOH | 19 |
| $CoS_x$/$Ni_3S_2$@NF | ~365 | 133 | 1.0 M KOH | 20 |
| Ni/$Mo_2C$(1:2)-NCNFs | 432 | 78.4 | 1.0 M KOH | 21 |
| FCC-Ni-NiS/NS-rGO | ~365 | 112 | 1.0 M KOH | 22 |
| Ni60Fe40-S/NSC | 385 | 30.9 | 1.0 M KOH | 23 |
| Ni-S-P | ~358 | 82 | 1.0 M KOH | 24 |
| $NiS_2$/$NiSe_2$ | ~400 | 119 | 1.0 M KOH | 25 |
| Ni-BDC@NiS | ~430 | 62 | 1.0 M KOH | 26 |
| S-CoO/$Co_3O_4$ | ~360 | 92 | 1.0 M KOH | 27 |
| $NiCo_2Se_4$ | 420 | 63 | 1.0 M KOH | 28 |
| NiFe–$NiFe_2O_4$ | ~400 | 74 | 1.0 M KOH | 29 |
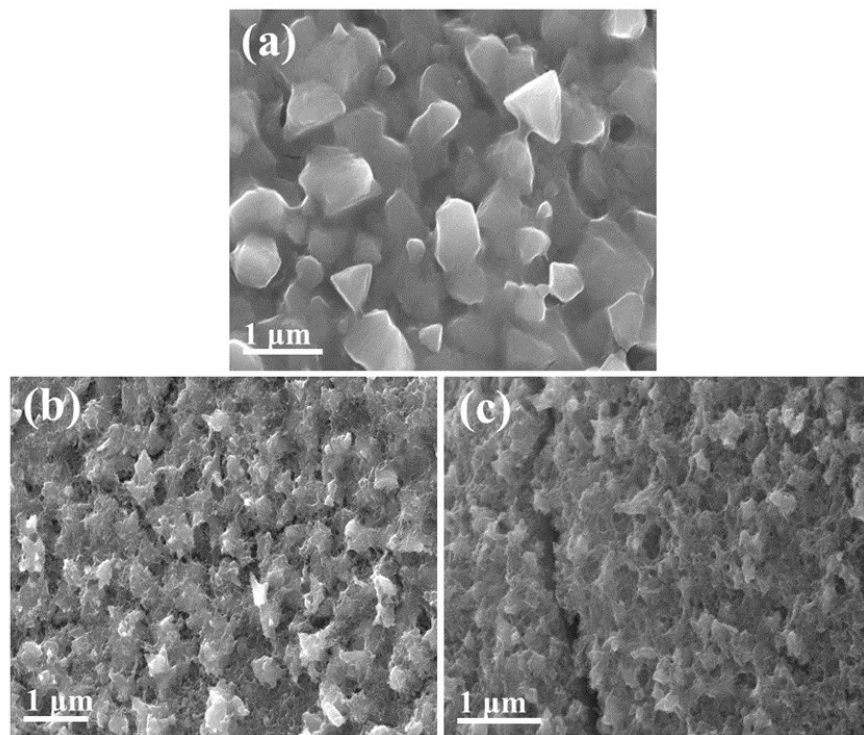
**Figure S5.** SEM images of (a) $MoS_2$-$Ni_3S_2$ (UR-1)/NF, (b) $MoS_2$-$Ni_3S_2$ (UR-2)/NF, (c) $MoS_2$-$Ni_3S_2$ (UR-3)/NF.

**Table S4.** The main parameters for evaluating the electrochemical activity of HER

| Catalysts | $\eta_{10}$ (mV) | $\eta_{100}$ (mV) | Tafel Slope (mV dec$^{-1}$) |
|---|---|---|---|
| $MoS_2$-$Ni_3S_2$ (UR-1)/NF | 98 | 181 | 74.8 |
| $MoS_2$-$Ni_3S_2$ (UR-2)/NF | 124 | 205 | 81.5 |
| $MoS_2$-$Ni_3S_2$ (UR-2)/NF | 132 | 224 | 84.3 |

**Table S5.** The main parameters for evaluating the electrochemical activity of OER.

| Catalysts | $\eta_{100}$ (mV) | Tafel Slope (mV dec$^{-1}$) |
|---|---|---|
| $MoS_2$-$Ni_3S_2$ (UR-1)/NF | 355 | 97.4 |
| $MoS_2$-$Ni_3S_2$ (UR-2)/NF | 388 | 116.3 |
| $MoS_2$-$Ni_3S_2$ (UR-3)/NF | 414 | 126.7 |

**Table S6.** Comparison of overall water splitting performance of $MoS_2$-$Ni_3S_2$ (UR-2)/NF with that of some recently reported bifunctional electrocatalysts in alkaline media.

| Catalysts | $\eta_{10}$ (V) | Electrolyte | Ref. |
|---|---|---|---|
| $MoS_2$-$Ni_3S_2$ (UR-2)/NF | 1.56 | 1.0 M KOH | This work |
| $Co_9S_8$ $Ni_3S_2$ HNTs/Ni | 1.59 | 1.0 M KOH | 10 |
| Co/β-$Mo_2C$@N-CNTs | 1.64 | 1.0 M KOH | 13 |
| O-CoMoS nanosheet | 1.60 | 1.0 M KOH | 14 |
| G-Mo-$Ni_3S_2$-2/NF | 1.58 | 1.0 M KOH | 15 |
| Co-$MoS_{1+X}Se_{1+Y}$1-5 | 1.60 | 1.0 M KOH | 17 |
| $CoS_x$/$Ni_3S_2$@NF | 1.572 | 1.0 M KOH | 20 |
| Ni/$Mo_2C$(1:2)-NCNFs | 1.64 | 1.0 M KOH | 21 |
| Ni-S-P | 1.58 | 1.0 M KOH | 24 |
| S-CoO/$Co_3O_4$ | 1.60 | 1.0 M KOH | 27 |
| ANF@NW | 1.71 | 1.0 M KOH | 30 |
| $NiSe_2$/3DSNG/NF | 1.59 | 1.0 M KOH | 31 |
| $CoS_x$/NCS | 1.83 | 1.0 M KOH | 32 |
| Cu-$NiS_2$ | 1.64 | 1.0 M KOH | 33 |
| Ar-$NiCo_2O_4$|S | 1.63 | 1.0 M KOH | 34 |
| CoP NFs | 1.65 | 1.0 M KOH | 35 |
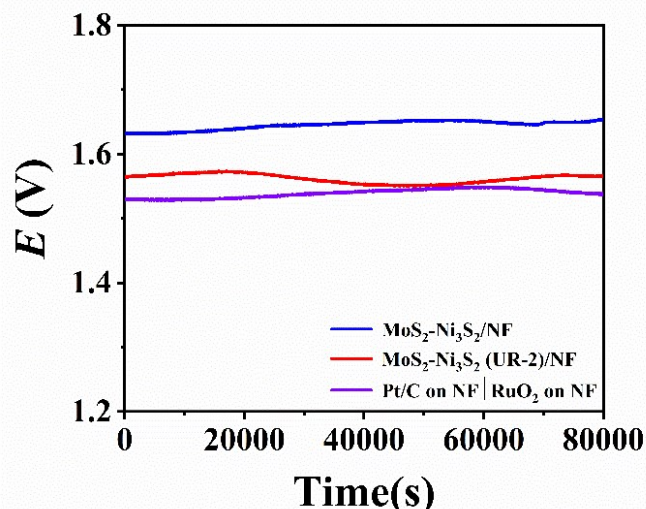
**Figure S6.** Stability tests at 10 mA cm$^{-2}$ of MoS$_2$-Ni$_3$S$_2$ (UR-2)/NF, Pt/C on NF|RuO$_2$

on NF and MoS$_2$-Ni$_3$S$_2$/NF for overall water splitting in an alkaline media (1.0 M

KOH).
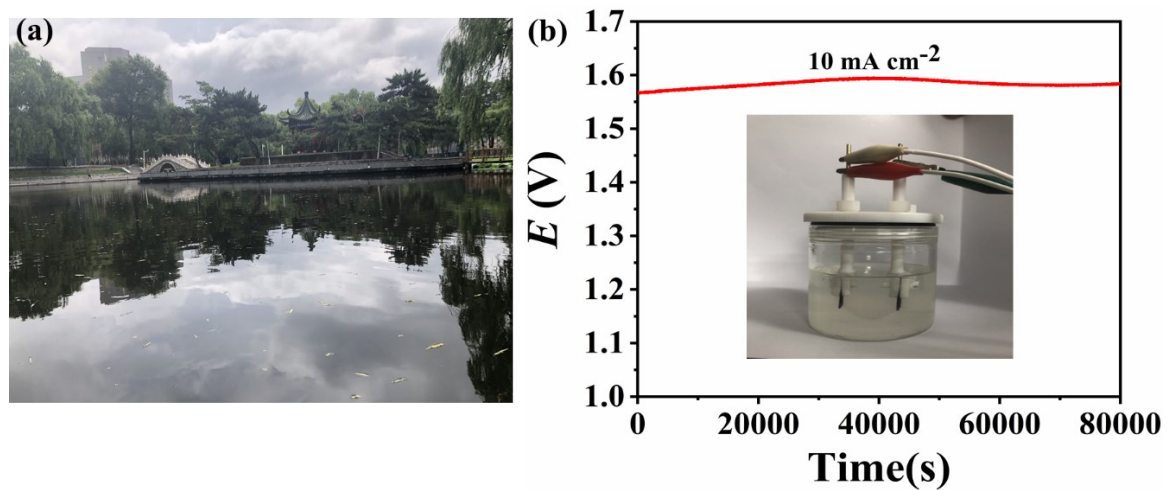


**Figure S7.** (a) Jing Lake (b) endurance tests at 10 mA cm$^{-2}$ of MoS$_2$-Ni$_3$S$_2$ (UR-2)/NF

for overall water splitting in grey water.
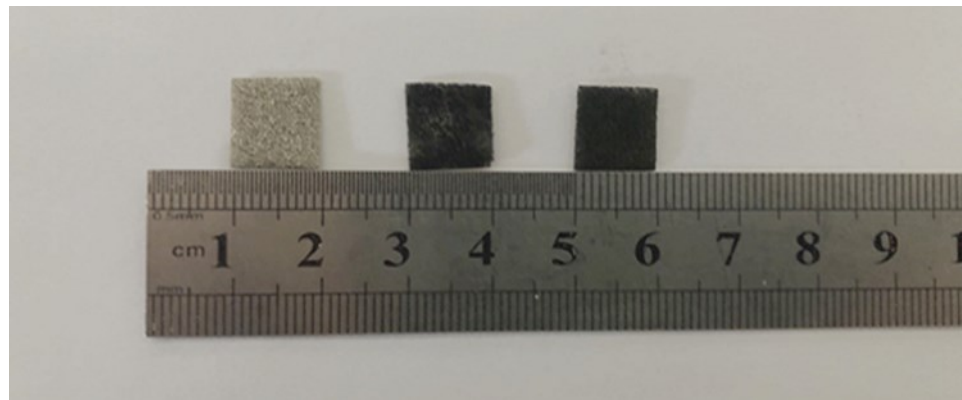


**Figure S8.** Photographs of (a) NF, (b) MoS$_2$-Ni$_3$S$_2$/NF and (c) MoS$_2$-Ni$_3$S$_2$ (UR-2)/NF.

**Table S7.** The main parameters for test and data analysis of the XRD

| Main parameters | Parameter settings |
|---|---|
| Instrument type | Siemens D5005 diffractometer |
| Source, photon energy | Cu-Kα, λ = 1.5418 Å, 40 kV and 30 mA |
| Scanning rate | 5 ° min$^{-1}$ |

| Geometry | $\theta\text{-}\theta$ |
|---|---|
| Measurement form | Bragg measurement |
| Type of detector | Array detector |
| Form of the sample | Self-supporting bulk material |
| Sample testing software | Smartlab guidance |
| Data analysis software | Jade6 |
| Drawing software | Origin 2018 |

**Table S8.** The main parameters for test and data analysis of the XPS

| Main parameters | Parameter settings |
|---|---|
| Instrument type | ESCALAB 250 spectrometer |
| Source, photon energy | Al Kα,1486.6 eV |
| Beam spot size | 500 μm |
| Scan mode | CAE |
| Whether it is a monochromatic source | monochromatic |
| Sample testing software | Avantage |
| Resolution | 0.5 eV |
| Form of the sample | Self-supporting bulk material |
| Data analysis software | XPS peak 4.1 |
| Background type of XPS peak 4.1 | Linear |
| %Lorentzian-Gaussian of XPS peak 4.1 | 80% |

| Drawing software | Origin 2018 |
|---|---|

**REFERENCES**

1.  J. Li, P. Xu, R. Zhou, R. Li, L. Qiu, S. P. Jiang and D. Yuan, $Co_9S_8$–$Ni_3S_2$ heterointerfaced nanotubes on Ni foam as highly efficient and flexible bifunctional electrodes for water splitting, *Electrochim. Acta*, 2019, **299**, 152-162.

2.  N. Jiang, Q. Tang, M. Sheng, B. You, D.-e. Jiang and Y. Sun, Nickel sulfides for electrocatalytic hydrogen evolution under alkaline conditions: a case study of crystalline NiS, $NiS_2$, and $Ni_3S_2$ nanoparticles, *Catal. Sci. Technol.*, 2016, **6**, 1077-1084.

3.  Z. Lin, Z. Wang, S. Shen, Y. Chen, Z. Du, W. Tao, A. Xu, X. Ye, W. Zhong and S. Feng, One-step method to achieve multiple decorations on lamellar $MoS_2$ to synergistically enhance the electrocatalytic HER performance, *J. Alloys Compd.*, 2020, **834**, 155217.

4.  S. Song, Y. Wang, W. Li, P. Tian, S. Zhou, H. Gao, X. Tian and J. Zang, Co-doped $Ni_3S_2$ hierarchical nanoarrays derived from zeolitic imidazolate frameworks as bifunctional electrocatalysts for highly enhanced overall-water-splitting activity, *J. Alloys Compd.* 2020, **827**, 154299.

5.  C. Tang, Z. Pu, Q. Liu, A. M. Asiri, Y. Luo and X. Sun, $Ni_3S_2$ nanosheets array supported on Ni foam: A novel efficient three-dimensional hydrogen-evolving electrocatalyst in both neutral and basic solutions, *Int. J. Hydrogen Energy*, 2015, **40**, 4727-4732.

6.  J. Zhang, T. Wang, D. Pohl, B. Rellinghaus, R. Dong, S. Liu, X. Zhuang and X. Feng, Interface engineering of $MoS_2$/$Ni_3S_2$ heterostructures for highly enhanced electrochemical overall-water-splitting activity, *Angew. Chem., Int. Ed.*, 2016, **55**, 6702-6707.

7.  H. Liang, L. Li, F. Meng, L. Dang, J. Zhuo, A. Forticaux, Z. Wang and S. Jin, Porous two-dimensional nanosheets converted from layered double hydroxides and their applications in electrocatalytic water splitting, *Chem. Mater.*, 2015, **27**, 5702-5711.

8.  Y. Qu, M. Yang, J. Chai, Z. Tang, M. Shao, C. T. Kwok, M. Yang, Z. Wang, D. Chua, S. Wang, Z. Lu and H. Pan, Facile synthesis of vanadium-doped $Ni_3S_2$ nanowire arrays as active electrocatalyst for hydrogen evolution reaction, *ACS Appl. Mater. Interfaces*, 2017, **9**, 5959-5967.

9.  T. Kou, T. Smart, B. Yao, I. Chen, D. Thota, Y. Ping and Y. Li, Theoretical and experimental insight into the effect of nitrogen doping on hydrogen evolution activity of $Ni_3S_2$ in alkaline medium, *Adv. Energy Mater.*, 2018, **8**, 1703538.

10. J. Li, P. K. Shen and Z. Tian, One-step synthesis of $Ni_3S_2$ nanowires at low temperature as efficient electrocatalyst for hydrogen evolution reaction, *Int. J.*

*Hydrogen Energy*, 2017, **42**, 7136-7142.

11. K. J. H. Lim, G. Yilmaz, Y.-F. Lim and G. W. Ho, Multi-compositional hierarchical nanostructured $Ni_3S_2$@$MoS_x$/NiO electrodes for enhanced electrocatalytic hydrogen generation and energy storage, *J. Mater. Chem. A*, 2018, **6**, 20491-20499.

12. X. Zhang, H. Xu, X. Li, Y. Li, T. Yang and Y. Liang, Facile synthesis of nickel–iron/nanocarbon hybrids as advanced electrocatalysts for efficient water splitting, *ACS Catal.*, 2015, **6**, 580-588.

13. T. Ouyang, Y. Q. Ye, C. Y. Wu, K. Xiao and Z. Q. Liu, Heterostructures composed of N-doped carbon nanotubes encapsulating cobalt and beta-$Mo_2C$ nanoparticles as bifunctional electrodes for water splitting, *Angew. Chem., Int. Ed.*, 2019, **58**, 4923-4928.

14. J. Hou, B. Zhang, Z. Li, S. Cao, Y. Sun, Y. Wu, Z. Gao and L. Sun, Vertically aligned oxygenated-$CoS_2$–$MoS_2$ heteronanosheet architecture from polyoxometalate for efficient and stable overall water splitting, *ACS Catal.*, 2018, **8**, 4612-4621.

15. J. Li, X. Zhang, Z. Zhang, Z. Li, M. Gao, H. Wei and H. Chu, Graphene-quantum-dots-induced facile growth of porous molybdenum doped $Ni_3S_2$ nanoflakes as efficient bifunctional electrocatalyst for overall water splitting, *Electrochim. Acta*, 2019, **304**, 487-494.

16. H. Yang, Y. Huang, W. Y. Teoh, L. Jiang, W. Chen, L. Zhang and J. Yan, Molybdenum selenide nanosheets surrounding nickel selenides sub-microislands on nickel foam as high-performance bifunctional electrocatalysts for water splitting, *Electrochim. Acta*, 2020, **349**, 136336.

17. Q. Zhou, X. Luo, Z. Liu, S. Li, Y. Nan, H. Deng, Y. Ma and W. Xu, Co-doped 1T′/T phase dominated $MoS_{1+X}Se_{1+Y}$ alloy nanosheets as bifunctional electrocatalyst for overall water splitting, *Appl. Surf. Sci.*, 2020, **513**, 145828.

18. X. Wang, Y. Xie, W. Zhou, X. Wang, Z. Cai, Z. Xing, M. Li and K. Pan, The self-supported Zn-doped CoNiP microsphere/thorn hierarchical structures as efficient bifunctional catalysts for water splitting, *Electrochim. Acta*, 2020, **339**, 135933.

19. J. Li, G. Wei, Y. Zhu, Y. Xi, X. Pan, Y. Ji, I. V. Zatovsky and W. Han, Hierarchical NiCoP nanocone arrays supported on Ni foam as an efficient and stable bifunctional electrocatalyst for overall water splitting, *J. Mater. Chem. A*, 2017, **5**, 14828-14837.

20. S. Shit, S. Chhetri, W. Jang, N. C. Murmu, H. Koo, P. Samanta and T. Kuila, Cobalt sulfide/nickel sulfide heterostructure directly grown on nickel foam: an efficient and durable electrocatalyst for overall water splitting application, *ACS Appl. Mater. Interfaces*, 2018, **10**, 27712-27722.

21. M. Li, Y. Zhu, H. Wang, C. Wang, N. Pinna and X. Lu, Ni strongly coupled with $Mo_2C$ encapsulated in nitrogen-doped carbon nanofibers as robust bifunctional catalyst for overall water splitting, *Adv. Energy Mater.*, 2019, **9**, 1803185.

22. M. B. Zakaria, Y. Guo, J. Na, R. Tahawy, T. Chikyow, W. A. El-Said, D. A. El-Hady, W. Alshitari, Y. Yamauchi and J. Lin, Layer-by-layer motif

heteroarchitecturing of N,S-Codoped reduced graphene oxide-wrapped Ni/NiS nanoparticles for the electrochemical oxidation of water, *ChemSusChem*, 2020, **13**, 3269-3276.

23.    X. He, X. Zhao, F. Yin, B. Chen, G. Li and H. Yin, NiS-FeS/N, S co-doped carbon hybrid: synergistic effect between NiS and FeS facilitating electrochemical oxygen evolution reaction, *Int. J. Energy Res.*, 2020, **44**, 7057-7067.

24.    Q. Xu, W. Gao, M. Wang, G. Yuan, X. Ren, R. Zhao, S. Zhao and Q. Wang, Electrodeposition of $NiS/Ni_2P$ nanoparticles embedded in amorphous $Ni(OH)_2$ nanosheets as an efficient and durable dual-functional electrocatalyst for overall water splitting, *Int. J. Hydrogen Energy*, 2020, **45**, 2546-2556.

25.    Y. Yang, Y. Kang, H. Zhao, X. Dai, M. Cui, X. Luan, X. Zhang, F. Nie, Z. Ren and W. Song, An interfacial electron transfer on tetrahedral $NiS_2/NiSe_2$ heterocages with dual-phase synergy for efficiently triggering the oxygen evolution reaction, *Small*, 2020, **16**, 1905083.

26.    P. He, Y. Xie, Y. Dou, J. Zhou, A. Zhou, X. Wei and J. R. Li, Partial sulfurization of a 2D MOF array for highly efficient oxygen evolution reaction, *ACS Appl. Mater. Interfaces*, 2019, **11**, 41595-41601.

27.    T. Sun, P. Liu, Y. Zhang, Z. Chen, C. Zhang, X. Guo, C. Ma, Y. Gao and S. Zhang, Boosting the electrochemical water splitting on $Co_3O_4$ through surface decoration of epitaxial S-doped CoO layers, *Chem. Eng. J.*, 2020, **390**, 124591.

28.    S. M. N. Jeghan and G. Lee, One-dimensional hierarchical nanostructures of $NiCo_2O_4$, $NiCo_2S_4$ and $NiCo_2Se_4$ with superior electrocatalytic activities toward efficient oxygen evolution reaction, *Nanotechnology*, 2020, **31**, 295405.

29.    R. A. Raimundo, V. D. Silva, E. S. Medeiros, D. A. Macedo, T. A. Simões, U. U. Gomes, M. A. Morales and R. M. Gomes, Multifunctional solution blow spun $NiFe–NiFe_2O_4$ composite nanofibers: structure, magnetic properties and OER activity, *J. Phys. Chem. Solids*, 2020, **139**, 109325.

30.    H. Sun, Z. Ma, Y. Qiu, H. Liu and G. G. Gao, Ni@NiO nanowires on nickel foam prepared via "acid hungry" strategy: high supercapacitor performance and robust electrocatalysts for water splitting reaction, *Small*, 2018, **14**, 1800294.

31.    J. Zhou, Z. Wang, D. Yang, F. Qi, X. Hao, W. Zhang and Y. Chen, $NiSe_2$-anchored N, S-doped graphene/Ni foam as a free-standing bifunctional electrocatalyst for efficient water splitting, *Nanoscale*, 2020, **12**, 9866-9872.

32.    Q. Ju, R. Ma, Y. Pei, B. Guo, Q. Liu, T. Zhang, M. Yang and J. Wang, Nitrogen-doped carbon spheres decorated with $CoS_x$ nanoparticles as multifunctional electrocatalysts for rechargeable zn-air battery and overall water splitting, *Mater. Res. Bull.*, 2020, **125**, 110770.

33.    K. N. Dinh, Y. Sun, Z. Pei, Z. Yuan, A. Suwardi, Q. Huang, X. Liao, Z. Wang, Y. Chen and Q. Yan, Electronic modulation of nickel disulfide toward efficient water electrolysis, *Small*, 2020, **16**, 1905885.

34.    J. H. Lin, Y. T. Yan, T. X. Xu, C. Q. Qu, J. Li, J. Cao, J. C. Feng and J. L. Qi, S doped $NiCo_2O_4$ nanosheet arrays by Ar plasma: an efficient and bifunctional electrode for overall water splitting, *J. Colloid Interface Sci.*, 2020, **560**, 34-39.

35.     L. Ji, J. Wang, X. Teng, T. J. Meyer and Z. Chen, CoP nanoframes as bifunctional electrocatalysts for efficient overall water splitting, *ACS Catal.*, 2019, **10**, 412-419.